Proteome analysis of lipofuscin in human retinal pigment epithelial cells

F. Schutt[a,b,*], B. Ueberle[c], M. Schnölzer[c], F.G. Holz[a], J. Kopitz[b]

[a] *Department of Ophthalmology, INF 400, D-69120 Heidelberg, Germany*
[b] *Department of Pathochemistry and Neurochemistry, University of Heidelberg, INF 220, D-69120 Heidelberg, Germany*
[c] *Protein Analysis Facility, German Cancer Research Center, INF 280, D-69120 Heidelberg, Germany*

Received 5 August 2002; accepted 15 August 2002

First published online 29 August 2002

Edited by Julio Celis

Abstract Excessive accumulation of lipofuscin in postmitotic retinal pigment epithelial cells is a common pathogenetic pathway in various blinding retinal diseases including age-related macular degeneration, which is now the most common cause of registerable blindness in the industrialized nations. To better understand the role of lipofuscin accumulation and to manipulate the pathogenetic mechanisms on both experimental and therapeutic levels we analyzed the proteome of isolated human ocular lipofuscin granules from human RPE cells. After homogenization and fractionation by gradient ultracentrifugation of the RPE/choroid complex from 10 pairs of human donors, protein compounds were separated by 2D gel electrophoresis and analyzed using matrix-assisted laser desorption/ionization mass spectrometry and HPLC-coupled electrospray tandem mass spectrometry. Besides a better understanding of downstream pathways, this approach may provide new targets for therapeutic interventions in a currently untreatable disease. **© 2002 Federation of European Biochemical Societies. Published by Elsevier Science B.V. All rights reserved.**

Key words: Lipofuscin; Proteome; Retinal pigment epithelium; Age-related macular degeneration

1. Introduction

Accumulation of lipofuscin is a common phenomenon in ageing cells [1]. In postmitotic retinal pigment epithelial (RPE) cells, lipofuscin accumulates with age and in association with various blinding retinal diseases including degenerative and hereditary entities [2,3]. Normal RPE cell function is an essential prerequisite for photoreceptor and, thus, neurosensory retinal function [4]. Lipofuscin composition is thought to vary to a large extent in different tissues including neuronal cells of the central nervous system or hepatocytes [1]. In human RPE cells, several lines of evidence indicate that lipofuscin is a potentially deleterious byproduct of the constant phagocytosis of shed distal photoreceptor outer segment (ROS) disks [5]. Normally, degradation of this phagocytic load throughout life occurs in the lysosomal compartment with subsequent release of degraded material at the basal cell side and clearance by the choriocapillaris [5]. The mechanisms of lipofuscinogenesis are currently incompletely understood. The occurrence in a variety of monogenetic retinal diseases such as Stargardt's disease (mutations in the ABCR gene) and Best's disease (mutations in the VMD2 gene) suggests that excessive accumulation of lipofuscin represents a common downstream pathogenetic pathway of various molecular etiologies [6,7]. There is both experimental and clinical evidence that lipofuscin in this particular cell phenotype is associated with cellular dysfunction and subsequent impairment of visual function in corresponding retinal areas [8,9]. In humans, photoreceptor density was found to correlate with the lipofuscin concentration of the apposing RPE cells [10]. In vivo investigations using confocal scanning laser ophthalmoscopy have demonstrated excessive lipofuscin accumulation in association with various manifestations of age-related macular degeneration (AMD) [11]. The development of atrophy has been found to occur in areas of increased lipofuscin-mediated fundus autofluorescence in a longitudinal study in patients with AMD [11]. Direct evidence that an individual component of lipofuscin interferes with metabolic functions of RPE cells has not been demonstrated until recently [12].

Electron microscopic studies have shown a stepwise conversion of lysosomal structures to lipofuscin granula. Although lysosomal hydrolytic enzymes are capable of degrading most cellular macromolecules, it is assumed that lipofuscin results from an incomplete degradation in secondary lysosomes and/or the presence of altered biomolecules that are not degradable [13]. Lipid oxidation has been suggested to play a role [14], whereby the pigments may arise as a consequence of antioxidant deficiency or under prooxidant conditions [15,16]. Once formed, the RPE cell has no means of degrading or transporting lipofuscin material and granules into the extracellular space via exocytosis. Subsequently, these granules are trapped in the cytoplasm. An age-dependent accumulation of RPE lipofuscin has been described applying various in vitro and in vivo methods [8,17].

Only few compounds of RPE lipofuscin have been identified to date [18]. Current knowledge suggests that lipofuscin is a heterogenous mixture of various biomolecules partially modified by oxidation and lipidperoxidation due to excessive UV-irradiation and high oxygen levels in the eye [19]. More than 10 different fluorophores have been identified [18]. A2-E (*N*-retinylidene-*N*-retinylethanolamine), a major retinoid component of RPE lipofuscin, which represents a Schiff base product of all-trans retinaldehyde and ethanolamine (ratio 2:1) has recently been shown to cause a striking inhibition of major lysosomal catabolic pathways in cultured human RPE cells in concentrations that occur in vivo [12,20,21]. While interference with normal cell function has been elucidated for A2-E, we speculate that lipofuscin granules may contain other potentially toxic compounds. Furthermore, an

*Corresponding author. Fax: (49)-6221-56 4228.
E-mail address: florian_schuett@med.uni-heidelberg.de (F. Schutt).

0014-5793/02/$22.00 © 2002 Federation of European Biochemical Societies. Published by Elsevier Science B.V. All rights reserved.
PII: S0014-5793(02)03312-4

expanded analysis of lipofuscin components may give insights into pathogenetic mechanisms and may, thus, provide new targets for designing effective therapeutic strategies in this currently untreatable blinding retinal disease. Therefore, we sought to determine the proteinous composition of isolated human ocular lipofuscin by applying modern protein analytical methods. To our knowledge this study represents the first description of the human lipofuscin proteome.

2. Materials and methods

2.1. Lipofuscin isolation

Lipofuscin was isolated using a procedure of Boulton et al. [22]. Briefly, the RPE/choroid complex of 10 pairs of eyes derived from donors of corneal transplantations with no known ophthalmologic disease aged between 61 and 97 years were collected and stored at −20°C. Post mortem times varied between 24 and 48 h. The cells of the complex were homogenized on ice in a Potter-Elvejem-Homogenizator using phosphate-buffered saline (PBSA) and centrifuged at 60×*g* for 7 min. to remove cellular debris. Then pigment granules were pelleted by centrifugation (6000×*g*/10 min.), resuspended in 4 ml 0.3 M sucrose, and layered on a discontinuous gradient built of eight different concentrations of sucrose: 2.0, 1.8, 1.6, 1.55, 1.5, 1.4, 1.2 and 1.0 M (4 ml each). Identification of pure lipofuscin in the first band was done by analysis of excitation and emission spectra of isolated lipofuscin as described by Boulton et al. [23] using the high performance spectralfluorometer SFM 25 (Kontron). The first orange-brown band between 1.0 and 1.2 M sucrose containing pure Lipofuscin was collected using a Pasteur pipet. Lipofuscin was resuspended in 0.3 M sucrose and purified on a second sucrose gradient. Dilution in PBSA, centrifugation at 6000×*g* for 10 min. and washing three times in PBSA followed. The samples were stored at −20°C.

2.2. Protein content of lipofuscin

Lipofuscin-related proteins were extracted from isolated lipofuscin with 0.5 M NaOH. Protein concentration was measured using the method of Lowry et al. applying bovine serum albumin as standard [24].

2.3. 2D gel electrophoresis of lipofuscin

Isoelectric focusing (IEF) was performed using dry polyacrylamide gel strips (IPG, 11 cm) with an immobilized pH gradient pH 3–10 and the IPGphor™ Isolectric Focusing System (Amersham Pharmacia Biotech). IPG strips were rehydrated in reswelling buffer [7 M urea, 2 M thiourea, 4% Triton X-100, 65 mM dithiothreitol (DTT), 0,8% Pharmalite] overnight. Lipofuscin protein was extracted in reswelling buffer and 80 μl were pipetted into the sample cup of each strip holder. The IEF protocol started at 100 V for 16 h followed by 500 V for 1 h, 500–8000 V (linear increase) within 10 h and finally 8000 V for 4.5 h.

The Multiphor II flatbed system and ExcelGel™, gradient 8–18 was used for sodium dodecylsulfate– polyacrylamide gel electrophoresis (SDS–PAGE) as second dimension. Equilibration buffer for IPG strips contained 50 mM Tris–HCl, pH8.5, 2% SDS, 6 M urea, 30% glycerol and 65 mM DTT for the first 15 min. followed by 260 mM iodoacetamide. After draining the equilibration solution on filter paper the IPG strips and prestained SDS–PAGE standards (Bio-Rad) were placed on the SDS gel. Electrical settings were 600 V, 20 mA, 30 W for 50 min, followed by increase of current up to 50 mA. The gel was finally stained with colloidal Coomassie G50 (Perbio) for 5 days [25].

2.4. Tryptic digestion

Protein spots were excised from the gel and washed twice with deionized water, 50% acetonitrile/water 1:1 and acetonitrile. Proteins were digested with 33–165 ng sequencing grade modified trypsin (Promega) in 40 mM ammonium bicarbonate at 37°C overnight. The reaction was stopped by freezing [25].

2.5. Matrix-assisted laser desorption ionization (MALDI) mass spectrometry

MALDI mass spectra were recorded in the positive ion reflector mode with delayed extraction on a Reflex II time-of-flight instrument (Bruker-Daltonik GmbH, Bremen, Germany) equipped with a SCOUT multiprobe inlet and a 337 nm nitrogen laser. Ion acceleration voltage was set to 26.5 kV, the reflector voltage was set to 30.0 kV and the first extraction plate was set 20.6 kV [25]. Mass spectra were obtained by averaging 200–300 individual laser shots. Calibration of the spectra was performed internally by a two-point linear fit using autolysis products of trypsin. Sample preparation for MALDI mass fingerprints was achieved by cocrystallization of matrix (α-cyano-4-hydroxy cinnamic acid) with ZipTip C18 (Millipore, Bedford, MA, USA) concentrated samples. Database search was done against the NCBInr database using the MASCOT search algorithm (www.matrixscience.com).

2.6. On-line high-performance liquid chromatography (HPLC)-coupled ESI MS/MS

LC separations of the tryptic digests were performed using a UltiMate Capillary/Nano-HPLC system (Dionex, Sunnyvale, CA, USA). After preconcentration using a 0.3 mm×1 mm C18 Pepmap column (LC-Packings, San Francisco, CA, USA), the peptide mixture was separated on a 75 μm ID×250 mm C18 Pepmap column (LC-Packings) with a flow rate of 190 nl/min and a linear gradient from 8 to 46% acetonitrile in 0.1% aqueous TFA in 55 min. The HPLC system eluent was connected to a Finnigan MAT LCQ ion trap mass spectrometer (ThermoFinnigan, San Jose, CA, USA) equipped with a nanospray source (Protana, Odense, Denmark). Spray voltage was set to 1.5 kV and heated capillary temperature was 200°C. After performing one scan in MS mode from 300 to 2000 Da, the three most intense ions in the scan were selected and subjected to CID. Database search was done using TurboSequest 2.0 (ThermoFinnigan, San Jose, CA, USA).

3. Results

Spectral characteristics of isolated lipofuscin corresponded to previously published spectra of pure RPE lipofuscin (Fig. 1) and light microscopic examination [22,23] of the purified granules confirmed their purity (data not shown). Extraction of lipofuscin isolated from 10 eyes yielded 18.9 mg of protein. 2D gel electrophoresis of extracted proteins resulted in the separation of 81 individual protein spots (Fig. 2). The spots were excised from the gel, digested with trypsin and analyzed by MALDI mass spectrometry. Proteins were subsequently identified by data base search with the obtained peptide mass fingerprints (Table 1). In addition, most of the samples

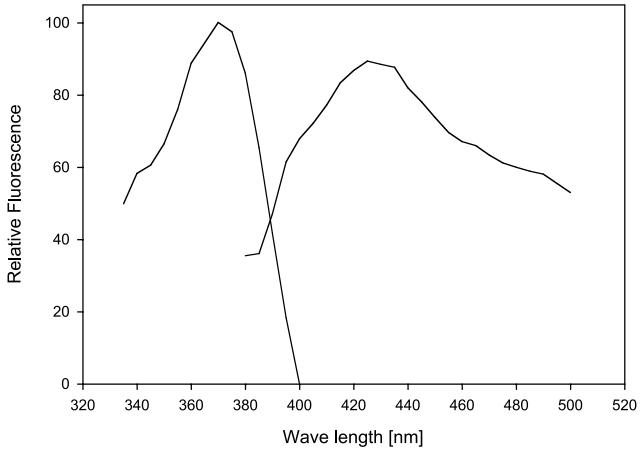

Fig. 1. Excitation and emission spectra of human ocular lipofuscin were recorded on a Kontron SFM 25 fluorimeter. The excitation spectrum was recorded at a constant emission wavelength of 430 nm. For recording of the emission spectrum, excitation was set at 360 nm. Spectra were corrected by subtracting measurements of pure solvent.

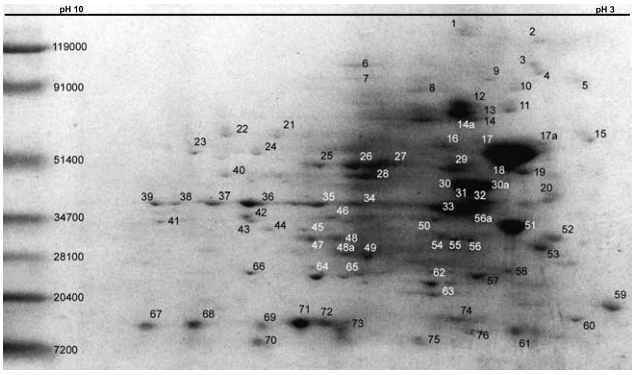

Fig. 2. Separation of lipofuscin proteins by 2D gel electrophoresis in an immobilized pH gradient from 3 to 10 with subsequent colloidal Coomassie staining as described in Section 2. Stained spots were identified by MALDI and ESI mass spectrometry and listed in Table 1 with corresponding numbers. Molecular weight markers (kDa) are shown at the left margin.

were also analyzed by HPLC-coupled ESI MS/MS to confirm the MALDI results by sequence data. Most of the identified proteins represent abundant cellular proteins, including cytoskeleton proteins, proteins of phototransduction, enzymes of metabolism, proteins of the mitochondrial respiratory chain, ion channel proteins and chaperones, which are known to occur in photoreceptors, RPE and other cell types. Remarkable is the occurrence of recoverin (spot 58), since it represents a photoreceptor cell-specific protein [26]. Four spots could not be identified due to missing database hits. Clusters of spots containing the same protein, e.g. spots 12–14, 34–36, 37–39, 47–49, 52–53, 55–56 and 63–65 may represent different post-translationally modified forms. For most of the spots the experimental molecular weight corresponded closely to the theoretical mass as deduced from the database. Only a few spots (20, 29, 31, 54, 57) indicated a lower molecular weight as compared to theoretical data, and one spot (49) exhibited a significantly higher experimental mass. Five spots were identified as hemoglobin chains probably representing blood contaminations during lipofuscin preparation.

4. Discussion

This is, to our knowledge, the first description of the protein components of human ocular lipofuscin isolated from RPE cells. Lipofuscin in postmitotic RPE cells is thought to be mainly a byproduct of the constant phagocytosis and degradation of shedded ROS. Therefore, lipofuscin should contain degradation products of photoreceptor-derived proteins. Indeed most of the identified protein components of lipofuscin have been shown to occur in photoreceptors, but many are also abundant in various other cell types, including RPE. The presence of the ROS-specific protein recoverin [26] underscores the contribution of phagocytosed ROS to lipofuscin. On the other hand, various mitochondria-derived proteins (e.g. in spots 18, 20, 23, 24, 27, 33, 40, 57, 60, 67, 75) were detected in lipofuscin granules, although ultrastructural examinations indicate that mitochondria are concentrated in photoreceptor inner segments, whereas ROS lack these organelles [27]. Thus a considerable proportion of lipofuscin is likely to originate from autophagic processes in the RPE cell itself.

The cytoplasmic space of aged RPE cells or cells with early excessive lipofuscin accumulation may be occupied by lipofuscin granules to large extend. It has been suggested that these vast intracellular deposits in membranous bags may physically impair cellular structure and function [28]. While it has initially been assumed that lipofuscin is merely an inert mixture of various biomolecules, several lines of evidence now indicate that it contains various cytotoxic compounds. Since the majority of the proteins identified herein are cellular house keeping proteins which per se would not be expected to have toxic properties, posttranslational modifications may result in generation of toxic substances. In particular, UV light in association with high oxygen concentrations causing permanent peroxidation of polyunsaturated lipids in the membrane system of photoreceptors finally may result in the generation of malondialdehyde (MDA) and 4-hydroxynonenal (4-HNE) which are known to modify proteins and initiate crosslinking. Such modification may hinder protein degradation by the lysosomal system, thereby contributing to lipofuscin deposition [13]. Furthermore, deposition of MDA- and 4-HNE-protein-adducts might be actively involved in the pathogenesis of AMD by inducing an inflammatory process [29]. Therefore, such posttranslational modifications of lipofuscin-associated proteins are currently investigated in our laboratory.

For most of the proteins identified, the molecular weight deduced from the position of the spots corresponded to the expected molecular weight. Therefore, intermolecular crosslinking of proteins to form higher complexes is unlikely. For some proteins (spots 20, 29, 31, 54, 57) the position in the gel was shifted to a lower molecular weight, probably indicating the accumulation of proteolytic degradation products in lipofuscin.

Opsin, the major protein component of ROS, was not detected in lipofuscin, suggesting that a high concentration of a protein in the phagocytosed material does not necessarily lead to its accumulation in lipofuscin granules.

The observation that human ocular lipofuscin contains several subunits of ATPase (spots 18, 23, 24, 57), interestingly, shows parallels to Batten disease (juvenile ceroid-lipofuscinosis), an inherited disorder which is characterized by massive lysosomal accumulations of subunit c of the mitochondrial ATP synthase complex. The disease results in total blindness due to retinal degeneration [30]. In an experimental model of the disease, accumulation of subunit c-containing autofluorescent lysosomal storage bodies is linked to severe retinal and neurologic degenerations [31].

Lipids, in particular carotenoids and retinoids, are also characteristic components of RPE lipofuscin and have been implicated in the pathogenesis of AMD. At present, the contribution of single compounds of lipofuscin to disease processes cannot yet be verified. A concerted action of various lipofuscin constituents appears likely. Our present study provides a starting point for further investigations on the potential role of the proteinous component of lipofuscin in the pathobiochemistry of various blinding retinal diseases including AMD.

Acknowledgements: Supported by Deutsche Forschungsgemeinschaft (DFG), Bonn, Germany: Schu 1388/2-1; Ho 1926/2-1, DFG-Research-Priority Program 'Age-related macular degeneration' (SPP 1088), State of Baden-Wuerttemberg Research Fund 500/2000.

Table 1
Proteome analysis of lipofuscin in human retinal RPE cells

Spot	Protein	NCBI	MW (kDa)
1	Hypothetical protein (alpha-spectrin homolog)	7512790	152.4
2	Not identified		
3	Tumor rejection antigen (gp96)	4507677	92.7
4	Tumor rejection antigen (gp96)	4507677	92.7
5	Not identified		
6	Hexokinase 1	15991833	102.2
7	Not identified		
8	Motor protein	5803115	84.0
9	Valosin-containing protein	6005942	90.0
10	Heat shock protein HSP 90-alpha (HSP 86)	123678	85.0
11	Heat shock 70 kDa protein 5	16507237	72.3
12	Annexin VI (Lipocortin VI)	113962	75.8
13	Annexin VI (Lipocortin VI)	113962	75.8
14	Annexin VI (Lipocortin VI)	113962	75.8
14a	Heat shock 70 kDa protein 8	5729877	70.8
15	Calreticulin precursor; Sicca syndrome antigen A	4757900	48.1
16	Tubulin, beta chain	5174739	49.6
	Prolyl-4-hydroxylase beta-subunit	2507460	57.0
17	Tubulin, alpha-1 chain	135395	50.8
17a	Tubulin beta chain	135448	50.2
18	ATP synthase beta chain	1145449	56.5
19	Enolase 2, gamma	5803011	47.6
20	Ubiquinol-cytochrome c reductase core protein I	4507841	53.3
21	Pyruvate kinase, muscle	14750405	58.5
22	Pyruvate kinase, muscle	14750405	58.5
23	ATP synthase, alpha subunit	4757810	59.7
24	ATP synthase, alpha subunit	4757810	59.7
25	Enolase 1, alpha	4503571	47.5
26	Enolase 1, alpha	4503571	47.5
27	S-arrestin	14737493	45.3
	NADH dehydrogenase Fe-S protein 2	4758786	52.5
28	Glutamate-ammonia ligase	15297214	42.7
	Tu translation elongation factor	4507733	49.5
	NADH dehydrogenase Fe-S protein 2	4758786	52.5
29	Serum albumin	28592	71.3
30	Creatin kinase	180570	42.9
30a	Beta actin	4501885	42.1
31	Vimentin	14742600	53.7
32	Guanine nucleotide-binding protein (0), alpha subunit 2	232134	40.6
33	Guanine nucleotide-binding protein, beta polypeptide 2	4885283	38.1
	Pyruvate dehydrogenase	2144337	39.2
34	Annexin A2	16306978	38.8
35	Annexin A2	16306978	38.8
36	Annexin A2	16306978	38.8
37	Glyceraldehyde-3-phosphate dehydrogenase	31645	36.2
38	Glyceraldehyde-3-phosphate dehydrogenase	31645	36.2
39	Glyceraldehyde-3-phosphate dehydrogenase	31645	36.2
40	Ubiquinol-cytochrome c reductase core protein II	14775827	48.6
41	Porin 31HM (anion channel 1)	238427	30.7
42	Voltage-dependent anion channel 2	4507881	32.1
43	Porin 31HM (anion channel 1)	238427	30.7
44	Not identified		
45	Voltage-dependent anion channel 2	4507881	32.1
46	Glyceraldehyde-3-phosphate dehydrogenase	31645	36.2
47	H119n carbonic anhydrase Ii	2554664	29.1
48	H119n carbonic anhydrase Ii	2554664	29.1
48a	Phosphoglycerate mutase 1	4505753	28.9
49	Crystallin, beta B2	4503063	23.5
50	Annexin IV	14738103	27.2
51	Annexin V (Lipocortin V)	999937	35.8
	Retinaldehyde binding protein 1	4506541	36.5
52	Tyrosine 3-monooxygenase/tryptophan 5-monoox. activation protein, epsilon	5803225	29.3
53	Tyrosine 3-monooxygenase/tryptophan 5-monoox. activation protein, theta	5803225	29.3
	Tyrosine 3-monooxygenase/tryptophan 5-monoox. activation protein, beta	4507949	28.1
	Tyrosine 3-monooxygenase/tryptophan 5-monoox. activation protein, zeta	4507953	27.7
54	Cathepsin D	4503143	45.0
55	Prohibitin	4505773	29.8
56	Prohibitin	4505773	29.8
56a	Cathepsin D	4503143	45.0
57	ATP synthase, subunit d	5453559	18.5
58	Recoverin	4506459	23.2

Table 1 (*Continued*).

Spot	Protein	NCBI	MW (kDa)
59	Calmodulin 2 (phosphorylase kinase, delta)	14250065	16.8
60	ATP synthase, H+transporting	4502297	17.4
61	Cytochrome c oxidase subunit Va precursor	4758038	16.9
62	Peroxiredoxin 2	13631440	22.0
63	Crystallin, alpha A	4503055	20.0
64	Crystallin, alpha B	4503057	20.1
65	Crystallin, alpha B	4503057	20.1
66	Neuropolypetide h3	9131159	21.0
67	Ubiquinol-cytochrome c reductase bindidng protein	5454152	13.5
	Hemoglobin alpha 2	4504345	15.3
68	Delta globin	4504351	16.2
69	Hemoglobin alpha 1 globin chain	13195586	10.7
70	Chain A, P11 (S100a10), ligand of annexin Ii	3212355	11.2
71	Mutant hemoglobin beta chain	18418633	16.1
72	Mutant hemoglobin beta chain	18418633	16.1
73	Mutant hemoglobin beta chain	18418633	16.1
74	Cellular retinoic acid binding protein 1	18314500	15.7
75	Cytochrome c oxidase subunit Vib	4502985	10.4
76	Glial fibrillary acidic protein	17479453	42.2

References

[1] Brizzee, K.R. and Ordy, J.M. (1981) in: Age Pigments (Sohal, R.S., Ed.), pp. 101–154, Elsevier, Amsterdam.
[2] Marmorstein, A.D., Marmorstein, L.Y., Sakaguchi, H. and Hollyfield, J.G. (2002) Invest. Ophthalmol. Vis. Sci. 43, 2435–2441.
[3] Mata, N.L., Weng, J. and Travis, G.H. (2000) Proc. Natl. Acad. Sci. USA 97, 7154–7159.
[4] Schraermeyer, U. and Heimann, K. (1999) Pigment Cell. Res. 12, 219–236.
[5] Kennedy, C.J., Rakoczy, P.E. and Constable, I.J. (1995) Eye 9, 763–771.
[6] Sun, H. and Nathans, J. (2001) J. Bioenerg. Biomembr. 33, 523–530.
[7] White, K., Marquardt, A. and Weber, B.H. (2000) Hum. Mutat. 15, 301–308.
[8] Holz, F.G., Bellmann, C., Staudt, S., Schutt, F. and Volcker, H.E. (2001) Invest. Ophthalmol. Vis. Sci. 42, 1051–1056.
[9] Shamsi, F.A. and Boulton, M. (2001) Invest. Ophthalmol. Vis. Sci. 42, 3041–3046.
[10] Wing, G.L., Gordon, C.B. and Weiter, J.J. (1978) Invest. Ophthalmol. Vis. Sci. 17, 601–609.
[11] Holz, F.G., Bellmann, C., Margaritidis, M., Schutt, F., Otto, T.P. and Volcker, H.E., Graefe's Arch. Exp. Clin. Ophthalmol. 237, 145–152.
[12] Holz, F.G., Schuett, F., Kopitz, J., Eldred, G.E., Kruse, F.E., Völcker, H.E. and Cantz, M. (1999) Invest. Ophthalmol. Vis. Sci. 40, 737–743.
[13] Katz, M.L. (1989) Adv. Exp. Med. Biol. 266, 109–116.
[14] Eldred, G.E. and Katz, M.L. (1991) Free Radic. Biol. Med. 10, 445–447.
[15] Handelman, G.J. and Dratz, E.A. (1986) Adv. Free Rad. Biol. Med. 2, 1–89.
[16] Anderson, R.E., Kretzer, F.L. and Rapp, L.M. (1994) Adv. Exp. Med. Biol. 366, 73–86.
[17] Delori, F.C., Dorey, C.K., Staurenghi, G., Arend, O., Goger, D.G. and Weiter, J.J. (1995) Invest. Ophthalmol. Vis. Sci. 36, 718–729.
[18] Eldred, G.E. and Katz, M.L. (1988) Exp. Eye Res. 47, 71–86.
[19] Berman, E.R. and Rothman, M.S. (1980) Am. J. Ophthalmol. 90, 783–791.
[20] Bermann, M., Schutt, F., Holz, F.G. and Kopitz, J. (2001) Exp. Eye Res. 72, 191–195.
[21] Holz, F.G., Bermann, M., Schutt, F. and Kopitz, J. (2002) Graefe's Arch. Exp. Clin. Ophthalmol., in press.
[22] Boulton, M. and Marshall, J. (1985) Exp. Eye Res. 41, 209–218.
[23] Boulton, M., Docchio, F., Dayhaw-Barker, P., Ramponi, R. and Cubeddu, R. (1990) Vis. Res. 30, 1291–1303.
[24] Lowry, O.H., Rosebrough, N.J. and Farr, A.L. (1951) J. Biol. Chem. 193, 265–275.
[25] Zatloukal, K., Stumptner, C., Fuchsbichler, A., Heid, H., Schnoelzer, M., Kenner, L., Kleinert, R., Prinz, M., Aguzzi, A. and Denk, H. (2002) Am. J. Pathol. 160, 255–263.
[26] McGinnis, J.F., Lerious, V., Pazik, J. and Elliott, R.W. (1993) Mamm. Genome 4, 43–45.
[27] Yamada, E. and Shikano, S. (1973) Electron Microscopic Atlas in Ophthalmology, Georg Thieme Publishers, Stuttgart, Tokyo.
[28] Feeney-Burns, L., Berman, E.R. and Rothman, H. (1980) Am. J. Ophthalmol. 90, 783–791.
[29] Hageman, G.S., Luthert, P.J., Victor Chong, N.H., Johnson, L.V., Anderson, D.H. and Mullins, R.F. (2001) Prog. Retin. Eye Res. 20, 705–732.
[30] Katz, M.L., Gao, C.-L., Prabhakaram, M., Shibuya, H., Liu, P.-C. and Johnson, G.S. (1997) Invest. Ophthalmol. Vis. Sci. 38, 2375–2386.
[31] Bronson, R.T., Lake, B.D., Cook, S., Taylor, S. and Davisson, M.T. (1993) Ann. Neurol. 33, 381–385.